Kinetik: Game Technology, Information System, Computer Network, Computing, Electronics, and Control
Journal homepage: http://kinetik.umm.ac.id
ISSN: 2503-2267
Vol. 11, No. 2, May, Pp. 391-402

Distributed secondary control with consensus-based adaptive droop and voltage observer for DC microgrids

Khusnul Hidayat[1,2], Arif Nur Afandi[*1]
Department of Electrical Engineering and Informatics, Universitas Negeri Malang, Indonesia[1]
Department of Electrical Engineering, Universitas Muhammadiyah Malang, Indonesia[2]

Article Info
Keywords:
DC Microgrid, Distributed Secondary Control, Consensus-based, Voltage Observer, Adaptive Droop

Article history:
Received: December 09, 2025
Accepted: March 10, 2026
Published: May 01, 2026

Cite:
K. Hidayat and A. N. Afandi, "Distributed Secondary Control with Consensus-Based Adaptive Droop and Voltage Observer for DC Microgrids", *KINETIK*, vol. 11, no. 2, May 2026.
https://doi.org/10.22219/kinetik.v11i2.2631

*Corresponding author.
Arif Nur Afandi
E-mail address:
an.afandi@um.ac.id

Abstract
This paper proposes a fully distributed secondary control scheme for a low-voltage DC microgrid with ring topology. The main objectives are to restore the common bus voltage to its nominal reference and to achieve accurate proportional current sharing among distributed generator units in the presence of non-uniform line resistances and mixed load conditions. The proposed secondary layer integrates a consensus-based adaptive droop controller and a consensus-based voltage observer. The adaptive droop mechanism dynamically adjusts the virtual impedance of each converter using neighbor-to-neighbor current information to reduce current-sharing errors, while the voltage observer provides a distributed estimate of the average bus voltage to compensate for droop-induced voltage deviations. The effectiveness of the proposed method is validated through simulation on a ring-configured DC microgrid consisting of four converters and five buses. A comparative study demonstrates that conventional droop control improves current sharing but introduces significant steady-state voltage deviation. By contrast, the proposed integrated approach achieves nearly zero current-sharing error while maintaining the DC bus voltage close to its reference value. The dynamic performance is further evaluated under both resistive-load and constant-power-load variations. The results show that the controller ensures fast voltage restoration, accurate proportional current sharing, and stable operation without sustained oscillations, even under nonlinear constant-power-load conditions. These findings indicate that the proposed distributed secondary control strategy provides robust voltage regulation and precise current sharing for ring-type DC microgrids.

1. Introduction

Low-voltage DC microgrids (DCMG) have emerged as an attractive solution for integrating distributed energy resources, storage units, and DC loads in applications such as data centers, electric vehicle charging stations, and residential nanogrids. In such systems, bus voltage regulation and accurate current sharing among distributed generators (DGs) are two fundamental yet often conflicting control objectives. A large body of work has investigated coordinated voltage regulation and current sharing in multi-bus DC microgrids, highlighting the inherent trade-offs imposed by line impedances, converter ratings, and control interactions [1], [2], [3], [4]. For example, compromised or multi-objective designs explicitly balance current-sharing accuracy against bus-voltage regulation performance [1], while distributed secondary controllers have been proposed to achieve both voltage restoration and optimal power sharing [2]. Other contributions focus on voltage-shifting and slope-adjusting strategies or average-voltage regulation schemes that rely only on current communication, further illustrating the importance of coordinated secondary control in DC microgrids [3], [4], [5].

Conventional droop control remains the de facto primary control method for DC microgrids because of its simplicity, plug-and-play capability, and suitability for decentralized implementation. However, the droop mechanism intrinsically introduces steady-state voltage deviations and is sensitive to non-uniform line impedances, making it difficult to simultaneously guarantee precise current sharing and tight voltage regulation. To alleviate these limitations, numerous droop-based enhancements have been proposed, including improved voltage-shifting strategies that explicitly couple bus-voltage deviation compensation with current-sharing objectives [5], game-theoretic formulations that minimize voltage-regulation deviations while enforcing accurate current sharing across multi-bus networks [6], and dynamic virtual-impedance schemes that modulate converter output impedance to mitigate ripple and improve robustness [7]. Additional studies extend distributed droop control to accommodate diverse load models (ZIP loads) and harsh operating conditions, demonstrating improved adaptability and stability under realistic scenarios [8]. Constant-power loads (CPLs) pose particular challenges because they can induce negative incremental impedance

and destabilize the system; recent work has therefore proposed distributed secondary controllers and enhanced droop schemes specifically tailored for near-infinite or tightly regulated CPLs [9].

Beyond primary droop enhancements, secondary control layers are widely employed to restore system voltages and refine current-sharing performance. To reduce communication burden and improve scalability, several researchers have adopted self-triggered and event-triggered communication mechanisms in distributed secondary control of DC microgrids. Discrete-time self-triggered controllers exploit prediction of triggering instants to cope with data dropouts and communication delays, while still ensuring average-voltage regulation and proportional current sharing [10]. Event-triggered schemes further reduce communication frequency by transmitting measurements only when certain error thresholds are exceeded, and have been used both for general DC microgrid stabilization [11] and for combined voltage-restoration and optimal power-sharing control in islanded DC networks [12]. The reliability of distributed secondary control under communication imperfections has also been analyzed, with dedicated strategies proposed to maintain stable operation and performance in the presence of packet loss, time-varying delays, and unreliable communication links [13]. In addition, convergence speed and performance guarantees have been strengthened through predefined-time and fixed-time secondary controllers that ensure bounded settling times under directed communication graphs or fully distributed architectures [14], [15], while further work has relaxed stability conditions for DC microgrids with CPLs, providing explicit upper bounds and design guidelines for stable operation under constant-power loading [16].

As distributed control architectures become more complex, robust stability and formal performance guarantees have received increasing attention. Several studies have analyzed the stability of DC microgrids under distributed controllers, deriving sufficient conditions for robust operation in the presence of parameter uncertainties and load variations [17], [18]. Distributed control strategies have also been extended to incorporate economic and operational objectives such as optimal coordination of conventional and renewable generators [19] and cooperative optimal secondary control using dynamic diffusion algorithms [20]. Consistency- or consensus-based formulations have been used to design control laws that guarantee coordinated voltage and power sharing while preserving network-wide consistency among local controllers [21]. These works collectively highlight the value of distributed secondary control in achieving system-level objectives such as voltage regulation, current sharing, and operational optimality without relying on centralized supervisory units.

More recently, advanced topics such as cyber–physical security, learning-based control, and multi-objective optimization have been incorporated into the distributed secondary control framework. Security-aware designs employ high-order differentiators and resilient estimation schemes to mitigate false data injection attacks in DC microgrids [22]. Learning-based methods, including multi-agent reinforcement learning, have been applied to secondary control to automatically discover control policies that can adapt to changing system conditions and uncertainties [23]. Predefined-time optimization frameworks and distributed optimal controllers explicitly address performance indices such as power-loss minimization, voltage deviation bounds, and convergence speed [24], [25]. Furthermore, fully distributed event-triggered strategies with adaptive observers have been proposed to enhance robustness and communication efficiency in renewable-powered DC microgrids [26], while robust observer-based secondary controllers have been developed to cope with parametric uncertainty and guarantee both voltage restoration and proportional load sharing [27].

Despite these extensive research efforts, several open challenges remain. Many existing schemes rely on relatively complex control architectures, require global information (such as centralized measurement of average bus voltage), or are tailored to specific microgrid topologies and load types. In particular, there is still a practical need for simple, fully distributed secondary control schemes that (i) operate with only neighbor-to-neighbor communication, (ii) can be implemented on standard droop-controlled converters, (iii) achieve simultaneous bus-voltage restoration and accurate current sharing under non-uniform line impedances, and (iv) are suitable for ring-configured multi-bus DC microgrids. Moreover, while several works employ consensus-based mechanisms, they often focus on either current sharing or voltage regulation, without a tight integration of a consensus-based voltage estimate with an adaptive droop law in a unified secondary-control framework.

Motivated by these gaps, this paper proposes a distributed secondary control scheme for a ring-type DC microgrid consisting of four DGs and five DC buses. The secondary control layer is composed of two consensus-based controllers: (1) a consensus-based adaptive droop controller that improves current-sharing accuracy by adaptively adjusting the virtual droop impedance based on neighbor current information, and (2) a consensus-based voltage observer that restores the DC bus voltage by compensating the voltage drop introduced by primary droop control. The scheme relies only on local measurements and neighbor-to-neighbor communication arranged in a ring topology, without any centralized coordination or global voltage measurement. The main contributions of this work can be summarized as follows:

1. A fully distributed secondary control architecture that combines an adaptive droop mechanism with a consensus-based voltage observer, enabling simultaneous current-sharing accuracy and voltage restoration in a droop-controlled DC microgrid.

2. A control design tailored to a ring-configured multi-bus DCMG with non-uniform line resistances and mixed local and common loads, demonstrating the applicability of consensus-based secondary control beyond simple single-bus configurations.
3. A comprehensive simulation study that compares the proposed method with conventional droop and non-adaptive secondary schemes, and evaluates its dynamic performance under load changes, showing that the proposed controller significantly reduces current-sharing error while keeping bus-voltage deviations small.

2. Research Method

This section describes the research method used to design and evaluate the proposed distributed secondary control applied to a low-voltage DCMG. The test system is a ring-shaped DCMG consisting of four distributed generators (DGs) and five DC buses, as depicted in Figure 1. The distributed secondary control is composed of two consensus-based controllers: 1) a consensus-based adaptive droop controller, which improves the accuracy of current sharing by adaptively adjusting the virtual droop impedance of each DG based on neighbor current information; and 2) a consensus-based voltage observer, which restores the DC bus voltage by compensating the voltage drop introduced by droop control.

Section 2.1 describes the electrical topology of the DCMG and the corresponding ring communication topology used for information exchange among DG controllers. Section 2.2 presents the consensus-based adaptive droop control for proportional current sharing. Section 2.3 then introduces the consensus-based voltage observer used for voltage restoration in the distributed secondary control layer.

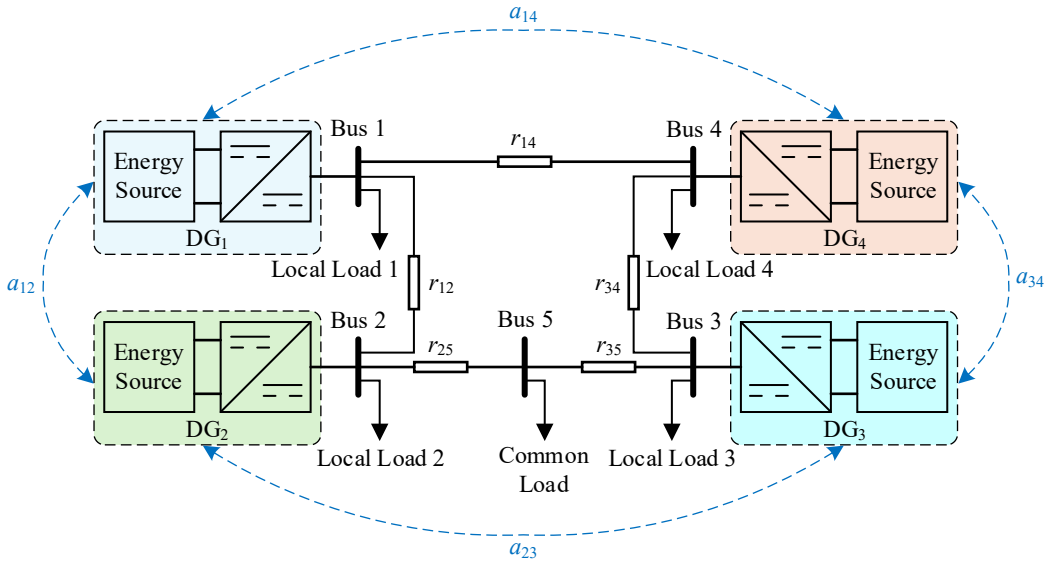

Figure 1. DC MG Structure with Multiple DGs and DC Buses

2.1 DC Microgrid and Communication Graph Model

The test system is a low-voltage DCMG with a ring bus topology, as shown in Figure 1. The electrical network consists of four DGs and five DC buses. Each DG unit consists of an energy resource and a DC–DC converter connected to one of the buses. Bus 1–Bus 4 are directly connected to DG1–DG4, respectively, and each of these buses supplies a local load. Bus 5 does not have a DG; it only supplies a common load. The buses are interconnected by distribution lines modeled as cable resistances.

In addition to the electrical network, a communication network is implemented among the DG controllers. The communication topology is also configured as a ring, in which each DG exchanges information only with its neighboring DGs. The communication network is represented by an undirected graph, as defined in Equation (1), where the set of nodes is given by Equation (2). Specifically, the node set represents the converters in the system, and each edge (DG_i, DG_j) $\in E_G$ denotes a bidirectional communication link between neighboring converters.

$$G = \{V_G, E_G\} \tag{1}$$

$$V_G = \{DG_1, DG_2, DG_3, DG_4\} \tag{2}$$

Based on the graph defined in (1)-(2), the corresponding adjacency matrix $A_G = [a_{ij}] \in \mathbb{R}^{N\times N}$ is constructed, where $a_{ij} = a_{ji} > 0$ if two converters are neighbors, and $a_{ij} = 0$ otherwise.

The degree matrix of the communication graph is then defined as shown in Equation (3), which captures the number of communication links associated with each node.

$$D_G = diag\left(\sum_{j=1}^{4} a_{1j}, \cdots, \sum_{j=1}^{4} a_{4j}\right) \tag{3}$$

Based on the adjacency and degree matrices, the Laplacian matrix is formulated as given in Equation (4), which plays a central role in the design of consensus-based control.

$$L_G = D_G - A_G \tag{4}$$

Because the communication graph is undirected, the Laplacian matrix L_G in (4) is symmetric and positive semidefinite, providing a suitable structure for consensus-based control design. Each DG controller uses this ring communication network to exchange voltage-observer and current-sharing information only with its neighbors, while the overall system objectives (accurate current sharing and voltage restoration) are achieved in a fully distributed manner.

2.2 Consensus-Based Adaptive Droop Control

The distributed secondary control has two main objectives: 1) to achieve accurate proportional current sharing among distributed sources; and 2) to support voltage restoration through coordination with the voltage observer. In this subsection, the focus is on consensus-based adaptive droop control, which specifically targets current-sharing accuracy by adaptively tuning the virtual impedance of each converter using neighbor-to-neighbor current information.

For converter *i*, the modified voltage reference applied to the inner voltage control loop is formulated as shown in Equation (5), where the droop term regulates current sharing while the correction term compensates for voltage deviations.

$$v_i^* = v_i^{ref} - v_i^d + \delta v_i = v_i^{ref} - r_i i_i + \delta v_i \tag{5}$$

where v_i^{ref} is the rated DC bus reference voltage, r_i is the virtual output impedance (droop coefficient) of converter i, $i_i(t)$ is the output current of converter i, and δv_i is the voltage correction term provided by the cooperative voltage regulator based on the consensus-based voltage observer (Section 2.3).

The droop term $r_i i_i(t)$ in Equation (5) improves current sharing but causes a steady-state voltage drop at the DC bus. Later, the correction signal $\delta v_i(t)$ will be used to compensate this drop and restore the voltage.

To improve current-sharing accuracy under unequal line impedances and parameter mismatches, the virtual impedance r_i is adapted using current information from other converters. The per-unit current mismatch at converter *i* is computed as defined in Equation (6), based on the differences between its normalized current and those of its neighboring converters.

$$\delta_i = \sum_{j \in N_i} a_{ij}\left(i_j^{pu} - i_i^{pu}\right) \tag{6}$$

where N_i is the set of converters that have direct communication links with converter i in the graph G. The per-unit current used in Equation (6) is defined as given in Equation (7).

$$i_i^{pu} = \frac{i_i}{I_i^{rated}} \tag{7}$$

with I_i^{rated} the rated current of converter i.

The mismatch δ_i is processed by a local PI controller $G_{3i}(s)$, producing an impedance correction term in the Laplace domain as expressed in Equation (8).

$$\Delta r_i = G_{3i}(s)\,\delta_i \tag{8}$$

The resulting correction signal is then used to update the virtual impedance as given in Equation (9).

$$r_i = r_{0i} - \Delta r_i \tag{9}$$

with r_{0i} denoting the initial droop coefficient based on the converter's rated current.

By continuously comparing per-unit currents with neighboring converters and updating $ri(t)$ according to Equation (6)–(9), the consensus-based adaptive droop control suppresses current-sharing errors and enforces proportional loading, even when line impedances are unequal or loads are time-varying. The implementation of the proposed distributed secondary control, including both the adaptive droop controller and the voltage observer, is illustrated in Figure 2.

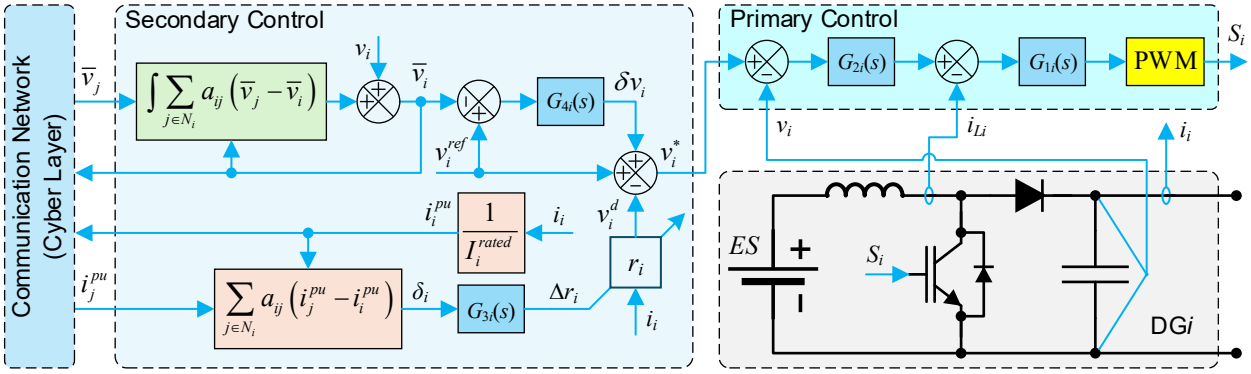

Figure 2. Implementation of the Proposed Distributed Secondary Control Method

2.3 Consensus-Based Voltage Observer

The consensus-based adaptive droop control described in Section 2.2 increases the accuracy of current sharing, but the droop mechanism in (5) inevitably causes a voltage drop at the DC bus. To restore the bus voltage to its nominal value, the distributed secondary control employs a consensus-based voltage observer. This observer provides each converter with a local estimate of the average DC bus voltage, which is then used to generate the voltage correction term $\delta v_i(t)$ in (5).

The observer at converter i uses the locally measured bus voltage $v_i(t)$; and the neighbor estimates $\bar{v}_j(t)$ received from converters $j \in N_i$. The observer implements a dynamic consensus protocol. In integral form, the update law of the consensus-based voltage observer is formulated as shown in Equation (10), where each converter updates its voltage estimate based on its local measurement and the exchanged information from neighboring units.

$$\bar{v}_i(t) = v_i(t) + \int_0^t \left[\sum_{j \in N_i} a_{ij} \left(\bar{v}_j(\tau) - \bar{v}_i(\tau) \right) \right] d\tau \tag{10}$$

The integral-form update law in Equation (10) can be equivalently expressed in differential form as Equation (11).

$$\dot{\bar{v}}_i(t) = v_i(t) + \sum_{j \in N_i} a_{ij} \left(\bar{v}_j(t) - \bar{v}_i(t) \right) \tag{11}$$

In Equation (11), the term $vi(t)$ allows the estimate $\bar{v}_i(t)$ to respond directly to variations in the local bus voltage, while the summation term forces the estimates of interconnected converters to move toward agreement. Under the connected, undirected communication graph described in Section 2.1, all $\bar{v}_i(t)$ converge to a common value that approximates the global average DC bus voltage.

The distributed estimate $\bar{v}_i(t)$ is then fed to the cooperative voltage regulator, which generates the correction signal $\delta v_i(t)$ in Equation (5). In this way, the consensus-based voltage observer compensates the voltage drop caused by droop control and performs voltage restoration, while the consensus-based adaptive droop control simultaneously maintains accurate current sharing—both implemented in a fully distributed secondary control framework.

2.4 Stability Analysis of the Proposed Distributed Secondary Control

To provide analytical insight into the stability of the proposed distributed secondary control scheme, the closed-loop error dynamics of the consensus-based adaptive droop controller and voltage observer are examined.

Let the per-unit current error vector be defined as given in Equation (12),

$$e_i = \frac{i_i}{I_{i,rated}} - \bar{i} \tag{12}$$

where $\bar{i}$ denotes the average per-unit current among the converters. By stacking all local errors in Equation (12), the global current error vector can be expressed as shown in Equation (13).

$$e = \left[e_1, e_2, \ldots, e_N\right]^T \tag{13}$$

Based on the consensus protocol structure, the adaptive droop update law can be expressed in compact form as given in Equation (14), which captures the closed-loop error dynamics.

$$\dot{e} = -K_r L_G e \tag{14}$$

where K_r is a positive definite diagonal gain matrix and L_G is the Laplacian matrix of the connected, undirected communication graph.

Since the graph is connected, L_G is symmetric positive semidefinite with a single zero eigenvalue corresponding to the consensus subspace. For all error vectors satisfying $1^T e = 0$, the reduced Laplacian is positive definite.

Consider the Lyapunov candidate function defined in Equation (15).

$$V = \frac{1}{2} e^T e \tag{15}$$

The time derivative of Equation (15) along system trajectories is obtained as shown in Equation (16).

$$\dot{V} = e^T \dot{e} = -e^T K_r L_G e \tag{16}$$

Because $K_r > 0$ and $L_G \geq 0$, it follows from Equation (16) that the inequality in Equation (17) holds.

$$\dot{V} \leq 0 \tag{17}$$

and $\dot{V} = 0$ only when $L_G e = 0$, which implies consensus. Therefore, the current-sharing error asymptotically converges to zero.

A similar argument applies to the voltage observer dynamics, which follow a standard dynamic average consensus protocol as described in Equation (18).

$$\dot{\bar{v}} = -K_v L_G \bar{v} + K_v \left(v - \bar{v}\right) \tag{18}$$

Under connected graph conditions and positive gains, the voltage estimation error converges asymptotically to zero.

Hence, the combined secondary control dynamics are stable in the Lyapunov sense, and proportional current sharing together with voltage restoration is guaranteed for the connected ring communication topology.

3. Results and Discussion

This section presents the simulation results and discusses the effectiveness of the proposed distributed secondary control scheme in a low-voltage DC microgrid. The performance is evaluated in terms of DC bus voltage regulation and current-sharing accuracy among four DGs under different operating conditions.

The system parameters used in the simulations are summarized in Table 1. The reference DC bus voltage is set to 100 V, while each DG is supplied by a 24 V energy resource through a DC–DC converter. The converter inductances and capacitances are selected as 2 mH and 220 μF, respectively, with a switching frequency of 10 kHz. The line resistances between buses are non-uniform (0.3–0.6 Ω), and the local loads connected to each DG bus range from 50 Ω to 70 Ω. The common load at Bus 5 is varied between 50 Ω, 90 Ω, and 70 Ω to emulate load changes in the microgrid.

Table 1. System Parameters

Parameters	Value
Reference Bus Voltage v_i^{ref}	100 V
Energy Resource Voltage V_{dc}	24 V
Converter inductance value L_i (i = 1, 2, 3, 4)	2 mH
Converter capacitance value C_i (i = 1, 2, 3, 4)	220 uF
Switching frequency f_{sw}	10 kHz
Line resistance r_{12}, r_{25}, r_{35}, r_{34}, r_{14}	0.3 Ω, 0.3 Ω, 0.4 Ω, 0.5 Ω, 0.6 Ω
Local load resistance R_{Li} (i = 1, 2, 3, 4)	50 Ω, 60 Ω, 50 Ω, 70 Ω
Common load resistance R_{CL}	50 Ω → 90 Ω, 90 Ω → 70 Ω

Two main test scenarios are considered: a) Scenario 1 (Figure 3) – comparative study of the conventional droop control and the proposed distributed secondary control, showing terminal voltages and supplied currents under four control stages; and b) Scenario 2 (Figure 4) – dynamic performance of the proposed consensus-based controller under step changes of the common load.

3.1 Scenario 1: Comparative Study Between Conventional Droop and Proposed Control

Figure 3 compares the behavior of the DC microgrid under: (i) operation without secondary control, (ii) conventional droop control, and (iii) the proposed consensus-based adaptive droop control combined with the consensus-based voltage observer. The results are shown in terms of terminal voltages (Figure 3(a)) and supplied currents (Figure 3(b)).

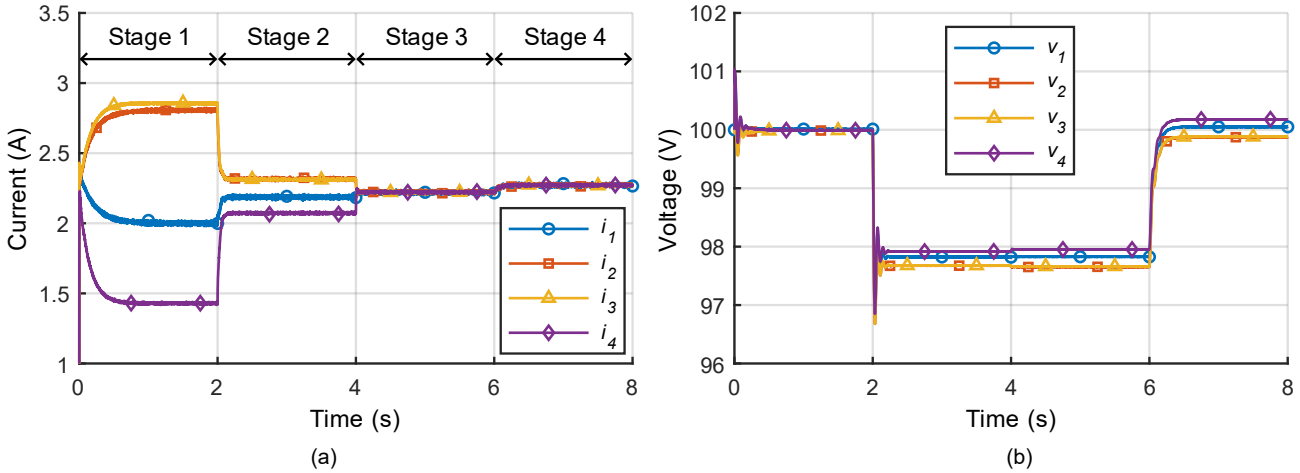

Figure 3. Comparative Studies of the Conventional Droop Control and the Proposed Control (a) Supplied Currents and (b) Terminal Voltages

Stage 1 (0 s – 2 s): without secondary control. In this interval, the secondary control (adaptive droop and voltage observer) is disabled. Each DG operates with its own local voltage control, so the DC bus voltage remains close to the reference value of 100 V. However, because the line resistances and load conditions are not identical, the DG currents differ significantly. This leads to a large current-sharing error, where some DGs are more heavily loaded than others, even though the bus voltage is well regulated.

Stage 2 (2 s – 4 s): conventional droop control enabled. In the second stage, conventional droop control is activated, while the proposed adaptive droop and voltage observer are still disabled. The introduction of droop control reduces the current-sharing error compared to Stage 1, because the DG terminal voltages are now adjusted as a function of their output currents. DGs supplying higher current experience a larger voltage drop, which tends to balance the load among the sources. Nevertheless, this comes at the cost of a noticeable voltage drop at the DC bus, so the

bus voltage deviates from the 100 V reference. Thus, conventional droop improves current sharing but introduces a steady-state voltage regulation error.

Stage 3 (4 s – 6 s): adaptive droop control enabled, observer disabled. In the third stage, the consensus-based adaptive droop control is activated, whereas the voltage observer remains disabled. The adaptive mechanism adjusts the virtual impedance of each DG based on neighbor-to-neighbor per-unit current comparisons. As a result, the currents supplied by the four DGs converge to their desired proportional values, and the current-sharing error becomes very small (close to zero). However, because the voltage observer is not yet active, the droop-induced voltage drop is not compensated, so the DC bus voltage still exhibits a significant deviation from the 100 V reference. In other words, this stage demonstrates that adaptive droop can achieve accurate current sharing, but voltage regulation remains unsatisfactory without secondary voltage restoration.

Stage 4 (6 s – 8 s): adaptive droop and voltage observer both enabled. In the final stage, both the consensus-based adaptive droop control and the consensus-based voltage observer proposed in this work are enabled. The adaptive droop continues to enforce proportional current sharing, while the voltage observer provides each DG with a distributed estimate of the average DC bus voltage, which is used to generate a correction term for the voltage reference. Under this combined control, the simulation results show that the current-sharing error remains very small (approximately zero) and, at the same time, the bus voltage deviation is significantly reduced, staying very close to the 100 V reference.

From Scenario 1, two important conclusions can be drawn: 1) Conventional droop control alone offers a trade-off: it improves current sharing but causes a noticeable voltage drop at the DC bus. 2) The proposed distributed secondary control—integrating consensus-based adaptive droop with a consensus-based voltage observer—successfully resolves this trade-off by simultaneously achieving accurate current sharing and good voltage regulation. This demonstrates the effectiveness of the proposed method in steady-state conditions under fixed load settings.

3.2 Scenario 2: Dynamic Performance Under Load Variations

This scenario evaluates the dynamic behavior and robustness of the proposed distributed secondary control under load disturbances. Two types of load conditions are investigated: (1) a resistive-load condition, where both local and common loads are purely resistive, and (2) a constant-power-load (CPL) condition, where local loads remain resistive while the common load is modeled as a CPL.

1) Resistive-Load Condition

In this simulation, all loads are resistive, and only the common load at Bus 5 is varied. Figure 4 presents the DG output currents and terminal voltages under step changes of the common load resistance.

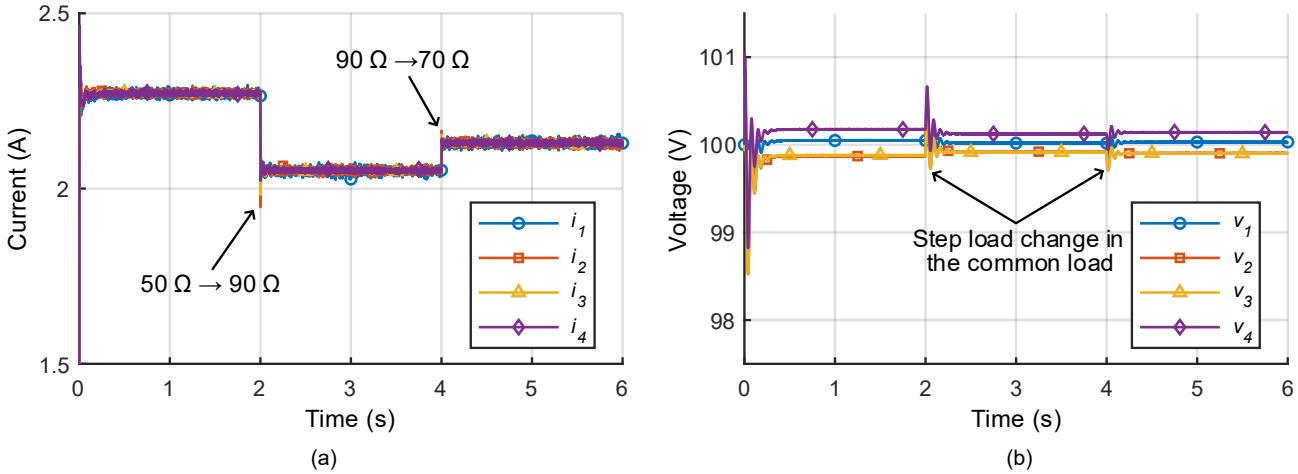

Figure 4. Dynamic Performance of the Proposed Distributed Secondary Control Under Resistive-load Variations: (a) DG Output Currents and (b) DG Terminal Voltages

The common load resistance is changed as follows: at t = 2 s, it increases from 50 Ω to 90 Ω; at t = 4 s, it decreases from 90 Ω to 70 Ω. An increase in resistance (50 Ω → 90 Ω) corresponds to a reduction in load demand, whereas a decrease in resistance (90 Ω → 70 Ω) corresponds to an increase in load demand.

When the load resistance increases at t = 2 s, the total current demand decreases. As a result, the DG output currents decrease accordingly. A small transient deviation in the terminal voltages is observed; however, the consensus-

based voltage observer rapidly compensates the disturbance, restoring the DC bus voltage close to its 100 V reference. The DG currents remain well balanced and proportional to their ratings during the transient and steady state.

At t = 4 s, when the load becomes heavier (90 Ω → 70 Ω), the DG currents increase to supply the additional demand. A temporary voltage dip occurs due to the sudden increase in load current, but the voltage is quickly restored. The current-sharing accuracy is preserved throughout the disturbance.

These results demonstrate that the proposed distributed secondary control maintains stable voltage regulation and accurate proportional current sharing under linear load variations.

2) Constant-Power-Load Condition

In the second experiment, the local loads remain resistive, while the common load at Bus 5 is modeled as a constant-power load (CPL). Compared with the resistive case, the CPL condition is more challenging because a CPL exhibits nonlinear characteristics and negative incremental impedance, which may reduce system damping and potentially degrade stability.

The CPL power is varied during the simulation to assess the dynamic robustness of the proposed controller. Specifically, at t = 2 s, the common load power decreases from 200 W to 100 W, and at t = 4 s, it increases again from 100 W to 150 W. Figure 5 illustrates the corresponding responses of the DG output currents, terminal voltages, and the common load power profile under these step changes.

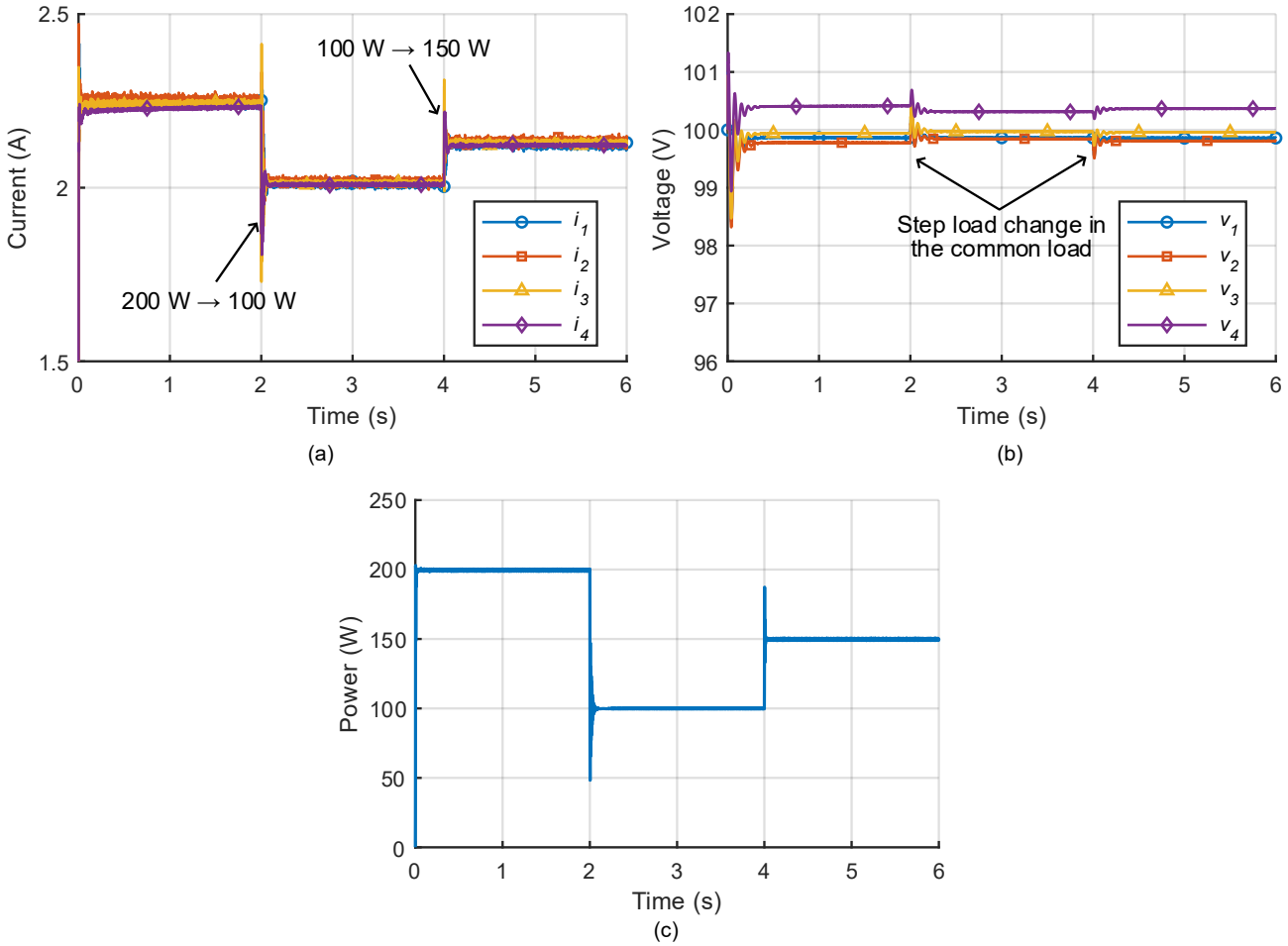

Figure 5. Dynamic Performance of the Proposed Distributed Secondary Control Under Constant-power-load (CPL) Variations: (a) DG Output Currents, (b) DG Terminal Voltages, and (c) Common Load Power

When the CPL power decreases at t = 2 s (200 W → 100 W), the total power demand from the DGs is reduced. Consequently, the DG output currents decrease proportionally. A small transient voltage deviation is observed immediately after the step change; however, the voltage observer rapidly generates a corrective signal that restores the bus voltage close to the nominal 100 V. The adaptive droop mechanism simultaneously maintains proportional current sharing, and the per-unit currents converge quickly to their desired values.

At t = 4 s, when the CPL power increases from 100 W to 150 W, the DGs must supply additional power. Because a CPL draws current inversely proportional to the bus voltage, this operating condition is more critical than the resistive-load case. A temporary voltage dip occurs following the step increase in load power. Nevertheless, the distributed voltage observer effectively compensates for the droop-induced voltage drop, and the bus voltage is restored within a short settling time. The DG currents increase accordingly while preserving proportional sharing among the converters.

Importantly, no sustained oscillations or instability are observed during either transition. Despite the nonlinear behavior of the CPL, the proposed distributed secondary control maintains stable operation, fast voltage recovery, and accurate current sharing.

Overall, the results under the constant-power-load condition confirm that the integration of consensus-based adaptive droop control and consensus-based voltage observer enhances system robustness against nonlinear load disturbances. Compared with the resistive-load experiment, the CPL case imposes stricter dynamic requirements; however, the proposed controller continues to ensure voltage regulation and proportional current sharing, validating its suitability for DC microgrids supplying converter-based loads.

4. Conclusion

This paper has proposed a fully distributed secondary control strategy for a low-voltage DC microgrid with ring topology, integrating a consensus-based adaptive droop controller and a consensus-based voltage observer. The proposed scheme was designed to simultaneously achieve accurate proportional current sharing and DC bus voltage restoration under non-uniform line resistances and mixed load conditions, while relying solely on neighbor-to-neighbor communication without centralized coordination.

The comparative study in Scenario 1 demonstrated that conventional droop control inherently involves a trade-off between current-sharing accuracy and voltage regulation. Although droop control improves load distribution among distributed generators, it introduces a steady-state voltage deviation. The activation of the consensus-based adaptive droop control significantly reduced current-sharing error by dynamically adjusting the virtual impedances of the converters. However, voltage deviation persisted until the consensus-based voltage observer was enabled. When both controllers operated simultaneously, the system achieved nearly zero current-sharing error while maintaining the DC bus voltage close to its nominal reference, effectively resolving the classical trade-off between these two control objectives.

In Scenario 2, the robustness of the proposed strategy was validated under both resistive-load and constant-power-load (CPL) variations. Under resistive load disturbances, the controller ensured fast voltage recovery and preserved proportional current sharing during transient conditions. More importantly, under CPL variations, where nonlinear behavior and negative incremental impedance impose stricter dynamic requirements, the proposed distributed secondary control maintained stable operation without sustained oscillations. The bus voltage was rapidly restored following step changes in load power, and accurate current sharing was preserved throughout the transitions. These results confirm that the integration of adaptive droop and distributed voltage estimation enhances system robustness not only under linear load changes but also under nonlinear and potentially destabilizing CPL conditions.

Overall, the simulation results indicate that the proposed distributed secondary control framework provides an effective and scalable solution for ring-type DC microgrids with non-uniform parameters and converter-based loads. The method achieves coordinated voltage regulation and current sharing using only local measurements and distributed communication, making it suitable for practical implementation. Future work will focus on experimental validation using a hardware prototype, extension to larger-scale and different network topologies, analysis under communication delays and packet losses, and integration with higher-level energy management and optimization layers.

References

[1] H. Bai, H. Zhang, H. Cai, and J. Schiffer, “Voltage regulation and current sharing for multi-bus DC microgrids: A compromised design approach,” *Automatica*, vol. 142, p. 110340, Aug. 2022. https://doi.org/10.1016/j.automatica.2022.110340

[2] Y. Dou, M. Chi, Z.-W. Liu, G. Wen, and Q. Sun, “Distributed Secondary Control for Voltage Regulation and Optimal Power Sharing in DC Microgrids,” *IEEE Trans. Control Syst. Technol.*, vol. 30, no. 6, pp. 2561–2572, Nov. 2022. https://doi.org/10.1109/TCST.2022.3156391

[3] S. Liu, H. Miao, J. Li, and L. Yang, “Voltage control and power sharing in DC Microgrids based on voltage-shifting and droop slope-adjusting strategy,” *Electr. Power Syst. Res.*, vol. 214, p. 108814, Jan. 2023. https://doi.org/10.1016/j.epsr.2022.108814

[4] P. S. Tadepalli, D. Pullaguram, and M. N. Alam, “DC Microgrid Average Voltage Regulation and Current Sharing With Solely Current Communication,” *IEEE J. Emerg. Sel. Top. Ind. Electron.*, vol. 6, no. 2, pp. 457–463, Apr. 2025. https://doi.org/10.1109/JESTIE.2024.3507088

[5] W. W. A. G. Silva, T. R. Oliveira, and P. F. Donoso-Garcia, “An Improved Voltage-Shifting Strategy to Attain Concomitant Accurate Power Sharing and Voltage Restoration in Droop-Controlled DC Microgrids,” *IEEE Trans. Power Electron.*, vol. 36, no. 2, pp. 2396–2406, Feb. 2021. https://doi.org/10.1109/TPEL.2020.3009619

[6] G. Yang, L. Ding, M. Ye, S. Xiao, and D. Yue, “Distributed Accurate Current Sharing for Multi-Bus DC Microgrids With Minimizing Voltage Regulation Deviations: A Game-Theoretic Approach,” *IEEE Trans. Smart Grid*, vol. 16, no. 4, pp. 2725–2737, Jul. 2025. https://doi.org/10.1109/TSG.2025.3553828

[7] S. Chaturvedi, D. Fulwani, and D. Patel, “Dynamic Virtual Impedance-Based Second-Order Ripple Regulation in DC Microgrids,” *IEEE J. Emerg. Sel. Top. Power Electron.*, vol. 10, no. 1, pp. 1075–1083, Feb. 2022. https://doi.org/10.1109/JESTPE.2021.3076474

[8] B. Fan, J. Peng, Q. Yang, and W. Liu, “Distributed Control of DC Microgrids With Improved ZIP Load Adaptability,” *IEEE Trans. Syst. Man Cybern. Syst.*, vol. 52, no. 7, pp. 4623–4633, Jul. 2022. https://doi.org/10.1109/TSMC.2021.3101813

[9] Z. Liu, L. Xing, J. Fang, Z. Shu, and H. Su, "Distributed Secondary Control for DC Microgrids With Near-Infinite Constant Power Load Accommodation," *IEEE Trans. Smart Grid*, vol. 16, no. 6, pp. 4451–4462, Nov. 2025. https://doi.org/10.1109/TSG.2025.3605924
[10] J. Peng, B. Fan, H. Xu, and W. Liu, "Discrete-Time Self-Triggered Control of DC Microgrids With Data Dropouts and Communication Delays," *IEEE Trans. Smart Grid*, vol. 11, no. 6, pp. 4626–4636, Nov. 2020. https://doi.org/10.1109/TSG.2020.3000138
[11] J. Peng, B. Fan, Q. Yang, and W. Liu, "Distributed Event-Triggered Control of DC Microgrids," *IEEE Syst. J.*, vol. 15, no. 2, pp. 2504–2514, Jun. 2021. https://doi.org/10.1109/JSYST.2020.2994532
[12] F. Guo, Z. Huang, L. Wang, and Y. Wang, "Distributed event-triggered voltage restoration and optimal power sharing control for an islanded DC microgrid," *Int. J. Electr. Power Energy Syst.*, vol. 153, p. 109308, Nov. 2023. https://doi.org/10.1016/j.ijepes.2023.109308
[13] H. Guo, X. Dai, S. Bu, and Z. Zhang, "Distributed Secondary Control of DC Microgrids Under Unreliable Communication Networks," *IEEE Trans. Autom. Sci. Eng.*, vol. 22, pp. 22900–22911, 2025. https://doi.org/10.1109/TASE.2025.3624598
[14] S. Chang, C. Wang, X. Luo, and X. Guan, "Distributed predefined-time secondary control under directed networks for DC microgrids," *Appl. Energy*, vol. 374, p. 123993, Nov. 2024. https://doi.org/10.1016/j.apenergy.2024.123993
[15] P. Wang, R. Huang, M. Zaery, W. Wang, and D. Xu, "A Fully Distributed Fixed-Time Secondary Controller for DC Microgrids," *IEEE Trans. Ind. Appl.*, vol. 56, no. 6, pp. 6586–6597, Nov. 2020. https://doi.org/10.1109/TIA.2020.3016284
[16] L. Xing, Z. Shu, J. Fang, C. Wen, and C. Zhang, "Distributed control of DC microgrids: A relaxed upper bound for constant power loads," *Automatica*, vol. 173, p. 112021, Mar. 2025. https://doi.org/10.1016/j.automatica.2024.112021
[17] Z. Liu and J. Li, "Robust Stability of DC Microgrid Under Distributed Control," *IEEE Access*, vol. 10, pp. 97888–97896, 2022. https://doi.org/10.1109/ACCESS.2022.3205615
[18] Z. Liu, J. Li, M. Su, X. Liu, and L. Yuan, "Stability Analysis of Equilibrium of DC Microgrid Under Distributed Control," *IEEE Trans. Power Syst.*, vol. 39, no. 1, pp. 1058–1067, Jan. 2024. https://doi.org/10.1109/TPWRS.2023.3266244
[19] Z. Fan, B. Fan, and W. Liu, "Distributed Control of DC Microgrids for Optimal Coordination of Conventional and Renewable Generators," *IEEE Trans. Smart Grid*, vol. 12, no. 6, pp. 4607–4615, Nov. 2021. https://doi.org/10.1109/TSG.2021.3094878
[20] B. Zhang, F. Gao, D. Liao, D. Liu, and P. W. Wheeler, "A Dynamic Diffusion Algorithm for Discrete-Time Cooperative Control for DC Microgrids," *IEEE Trans. Power Electron.*, vol. 39, no. 8, pp. 9399–9414, Aug. 2024. https://doi.org/10.1109/TPEL.2024.3395998
[21] N. Zhang, D. Yang, H. Zhang, and Y. Luo, "Distributed control strategy of DC microgrid based on consistency theory," *Energy Rep.*, vol. 8, pp. 739–750, Nov. 2022. https://doi.org/10.1016/j.egyr.2022.05.189
[22] Y. Jiang, Y. Yang, S.-C. Tan, and S. Y. R. Hui, "A High-Order Differentiator Based Distributed Secondary Control for DC Microgrids Against False Data Injection Attacks," *IEEE Trans. Smart Grid*, vol. 13, no. 5, pp. 4035–4045, Sep. 2022. https://doi.org/10.1109/TSG.2021.3135904
[23] F. Li *et al.*, "Distributed secondary control for DC microgrids using two-stage multi-agent reinforcement learning," *Int. J. Electr. Power Energy Syst.*, vol. 164, p. 110335, Mar. 2025. https://doi.org/10.1016/j.ijepes.2024.110335
[24] Y.-W. Wang, Y. Zhang, X.-K. Liu, and X. Chen, "Distributed Predefined-Time Optimization and Control for Multi-Bus DC Microgrid," *IEEE Trans. Power Syst.*, vol. 39, no. 4, pp. 5769–5779, Jul. 2024. https://doi.org/10.1109/TPWRS.2023.3349165
[25] Z. Fan, B. Fan, J. Peng, and W. Liu, "Operation Loss Minimization Targeted Distributed Optimal Control of DC Microgrids," *IEEE Syst. J.*, vol. 15, no. 4, pp. 5186–5196, Dec. 2021. https://doi.org/10.1109/JSYST.2020.3035059
[26] H. Saeidi, N. Mahdian Dehkordi, and H. Karimi, "Dynamic Threshold-Based Event-Triggered Strategy for Robust Fully Distributed Control in Renewable-Powered DC Microgrids," *IEEE Trans. Consum. Electron.*, vol. 71, no. 4, pp. 9689–9701, Nov. 2025. https://doi.org/10.1109/TCE.2025.3599935
[27] J. Lee and J. Back, "Distributed Robust Secondary Controller for Voltage Balancing and Proportional Load Sharing in Uncertain DC Microgrids," *IEEE Access*, vol. 12, pp. 91011–91024, 2024. https://doi.org/10.1109/ACCESS.2024.3409740